

Supporting Information

Tunable Photoluminescence in Flexible Carboxylate Ligands-Based Coordination Polymers with Interesting Topologies and Fe³⁺ Sensitivity.

Man-Ting Chen,^a Xiao-Dan Xie,^a Jin-Xiu Meng,^a Yong-Cong Ou,^a Jian-Zhong Wu,^b Ming-Liang Tong^c

^a *Guangzhou Key Laboratory of Materials for Energy Conversion and Storage, School of Chemistry, South China Normal University, Guangzhou 510006, China. Email: ouyongcong@m.scnu.edu.cn*

^b *Key Laboratory of Theoretical Chemistry of Environment, Ministry of Education, School of Chemistry, South China Normal University, Guangzhou 510006, China. Email: wujzh@scnu.edu.cn*

^c *Key Laboratory of Bioinorganic and Synthetic Chemistry of Ministry of Education, School of Chemistry, Sun Yat-Sen University, Guangzhou 510275, China.*

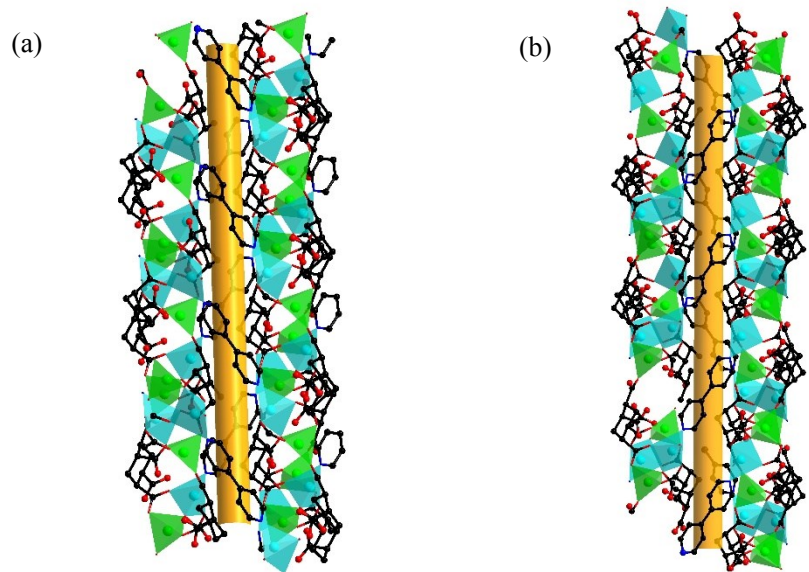


Figure S1. left-handed (a) and right-handed (b) helical structures along *b*-axis in **2**.

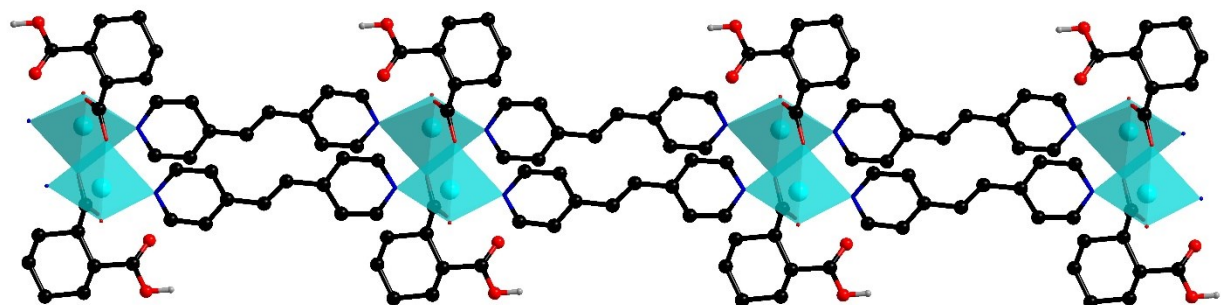


Figure S2. Polyhedron view of the 1D double-stand ladder-like chain in **5**.

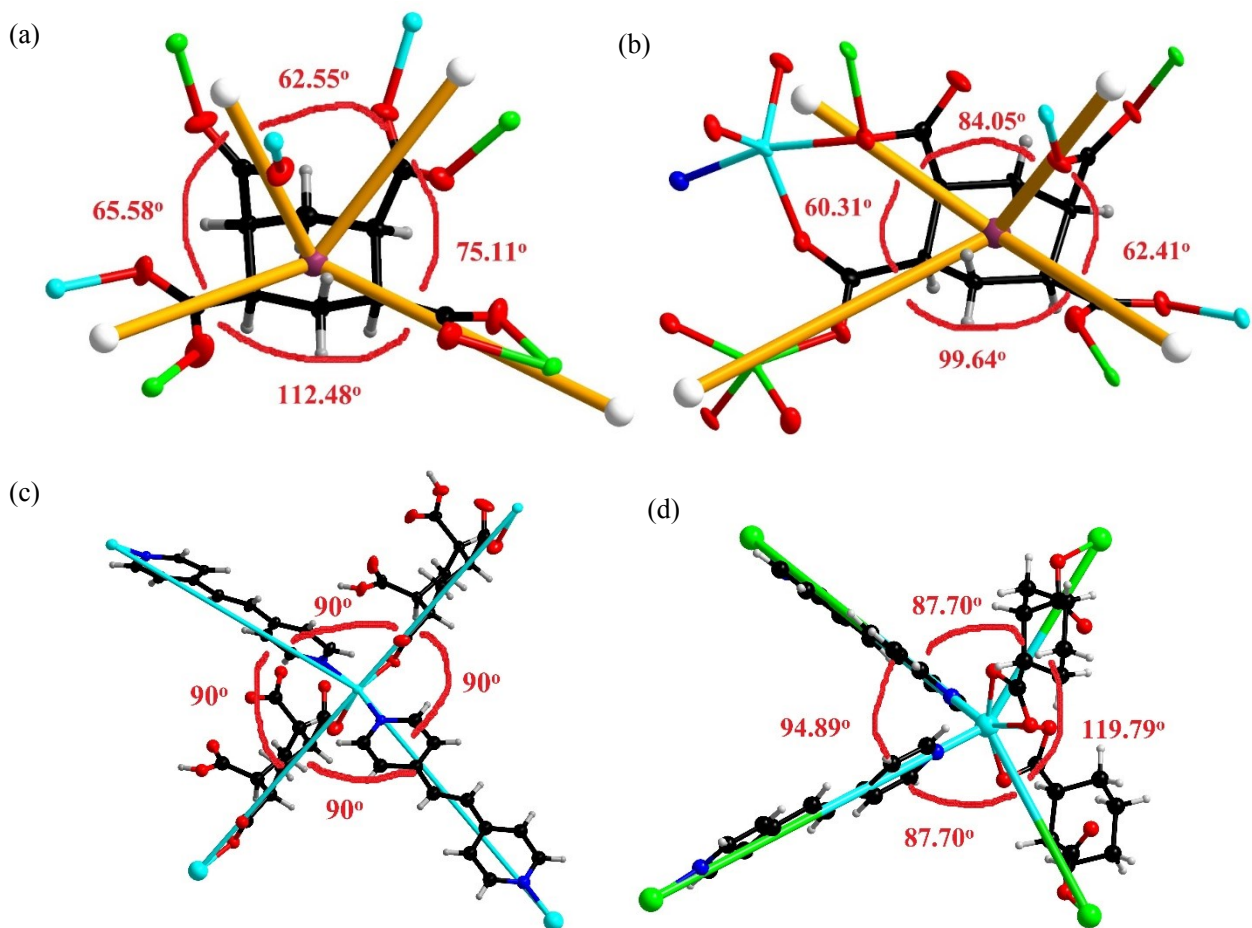


Figure S3. The bonding angles of four-connected nodes in **1(a)**, **2(b)**, **3(c)** and **4(d)**. The purple and white balls both in (a) and (b) represent central points of cyclohexane ring in chtc^{4+} ligand and dinuclear units respectively.

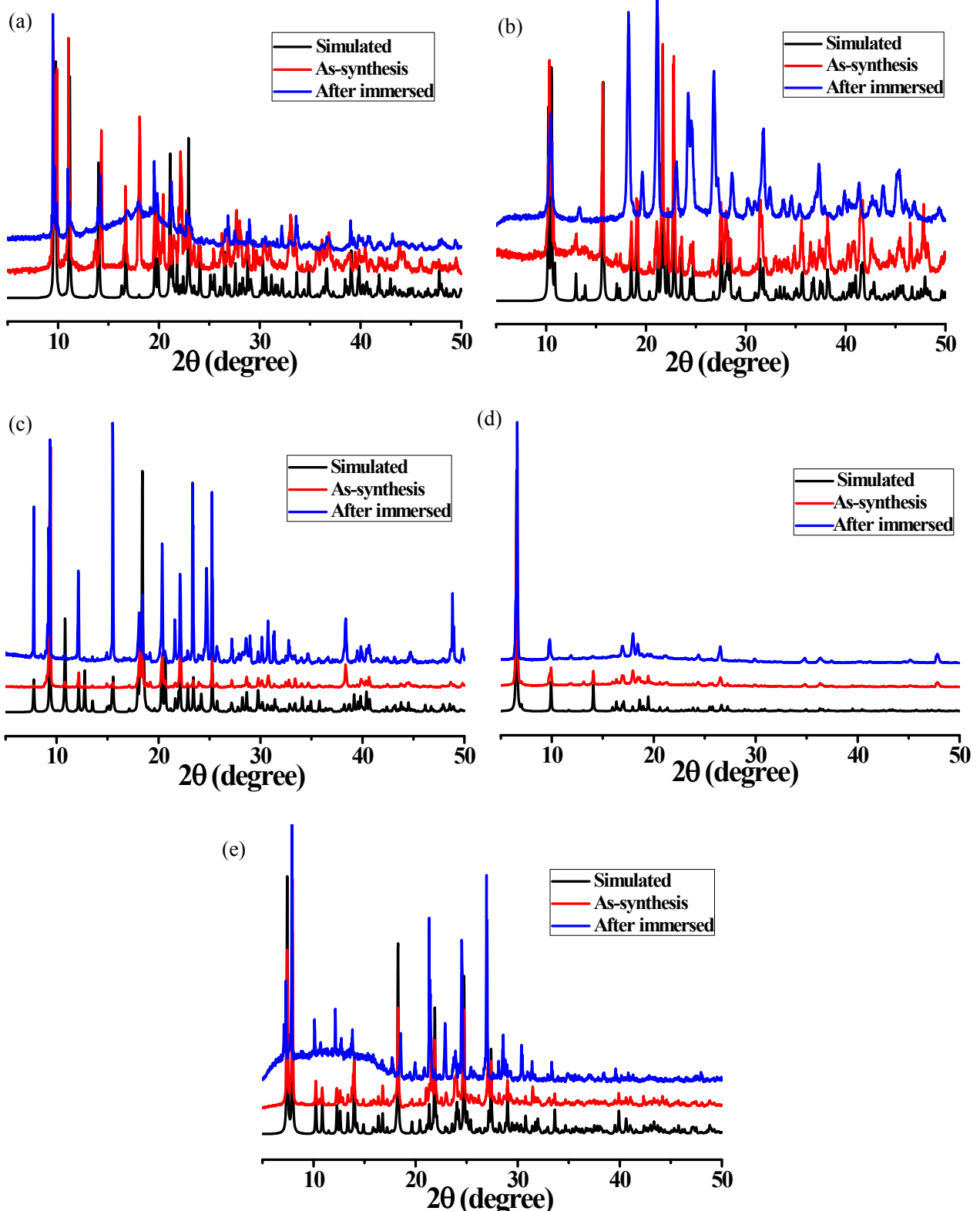


Figure S4. The PXRD patterns of complexes **1** (a), **2**(b), **3** (c), **4** (d) and **5** (e) before (red) and after (blue) immersed in water solution with Fe^{3+} ion.

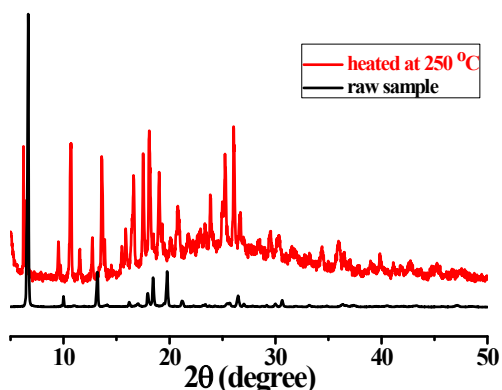


Figure S5. The PXRD patterns of complex **4** before and after heated at 250 °C under N₂ atmosphere. The peaks after desolvation obviously moved and different from the raw sample, indicating the crystal lattice was changed. We envisioned that it resulted from the movement of the interpenetrated frameworks.

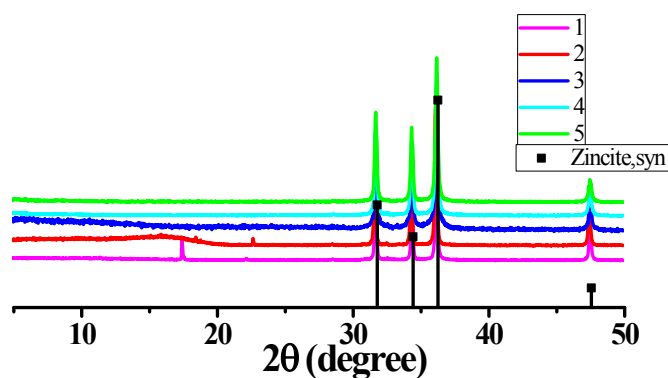


Figure S6. PXRD patterns for the decomposed samples 1-5 and the black drop lines represented the diffraction peaks of zincite (PDF#36-1451).

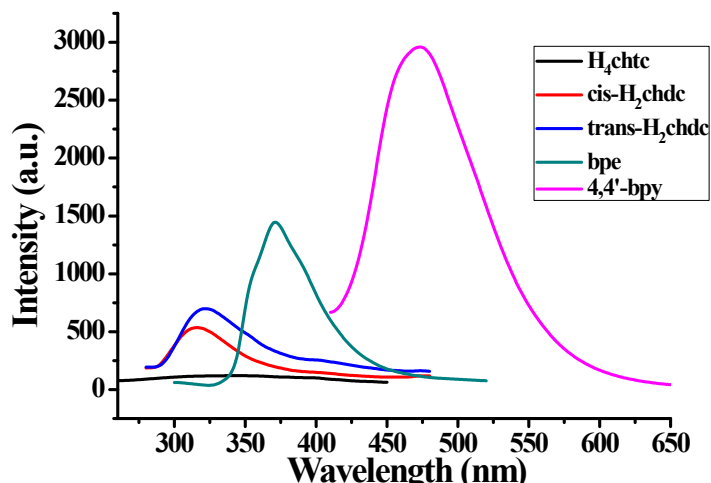
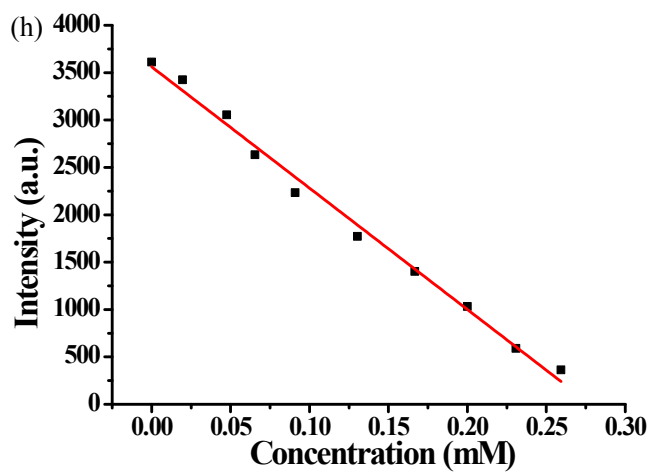
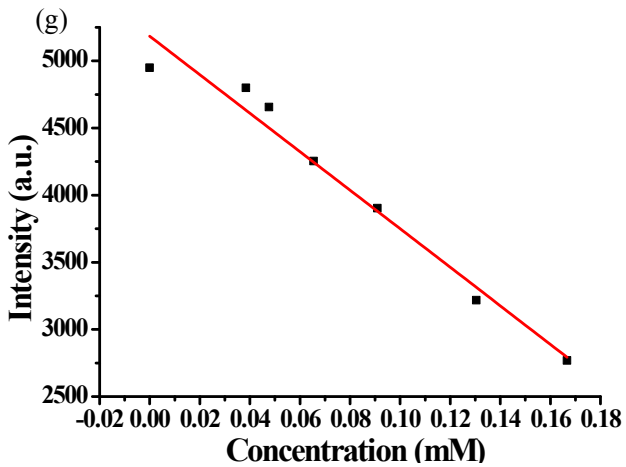
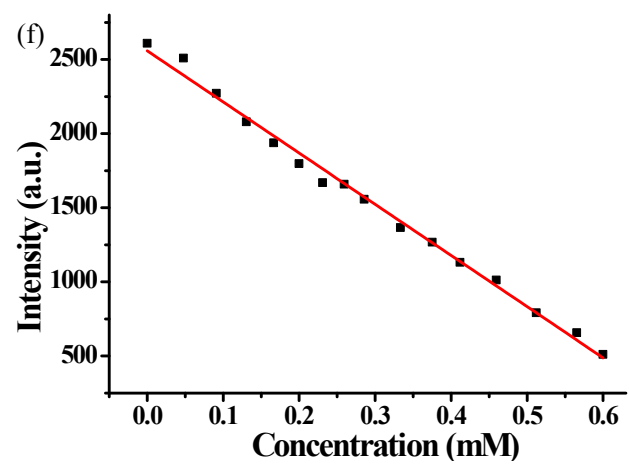
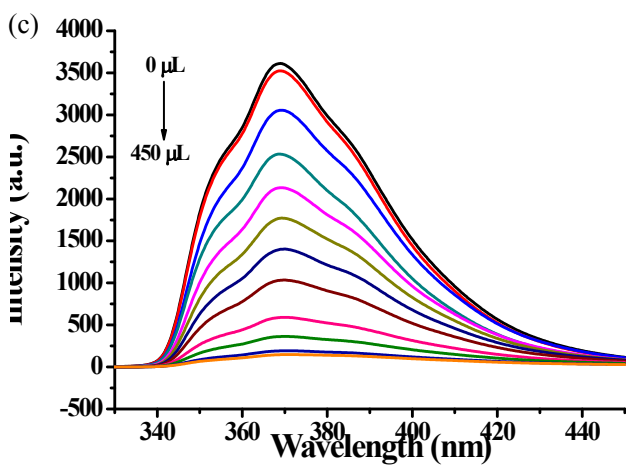
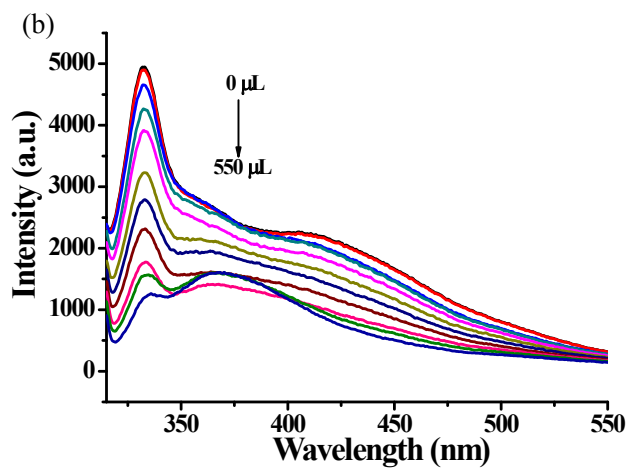
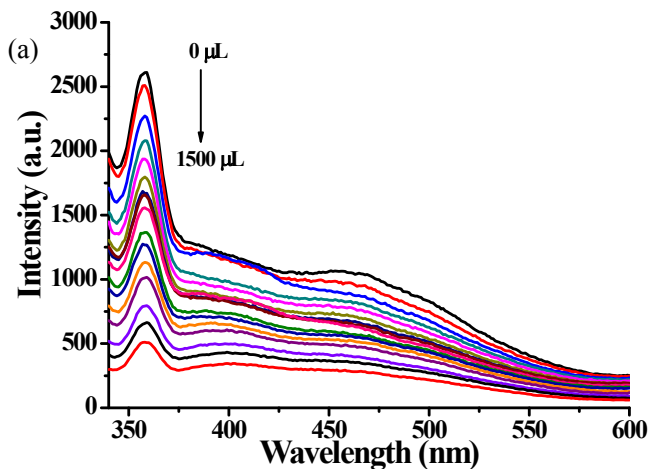


Figure S7. The emission spectra with excitation at 240nm, 250 nm, 252 nm, 282 nm and 387 nm for H₄chtc, cis-H₂chdc, trans-H₂chdc, bpe and 4,4'-bpy respectively.



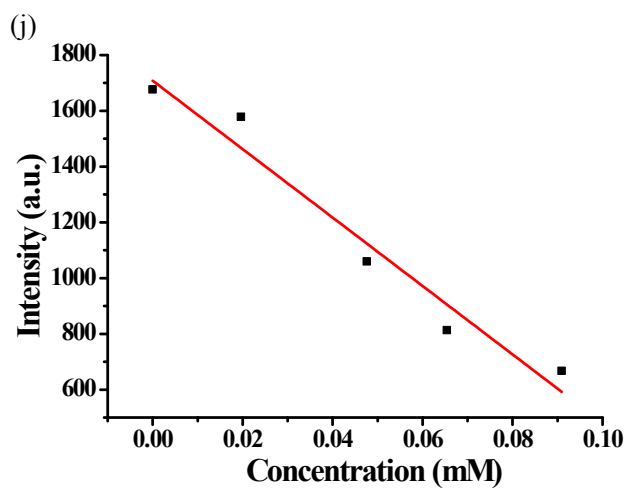
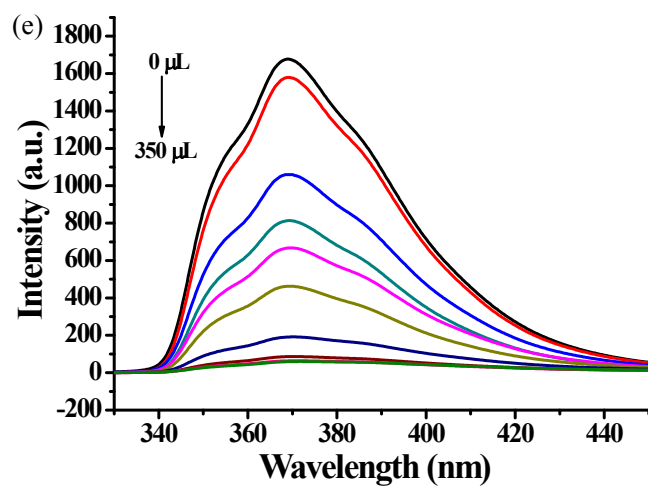
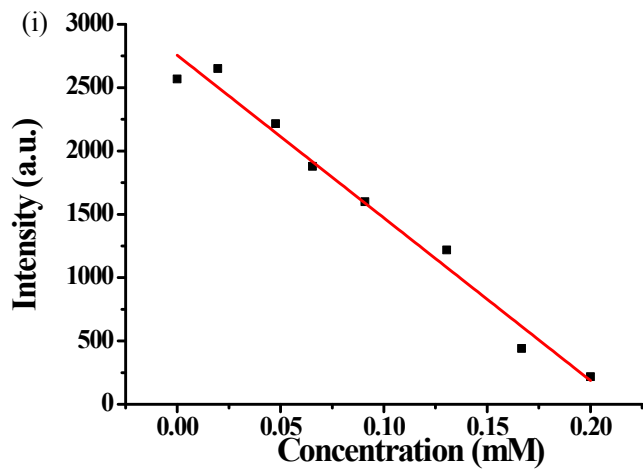
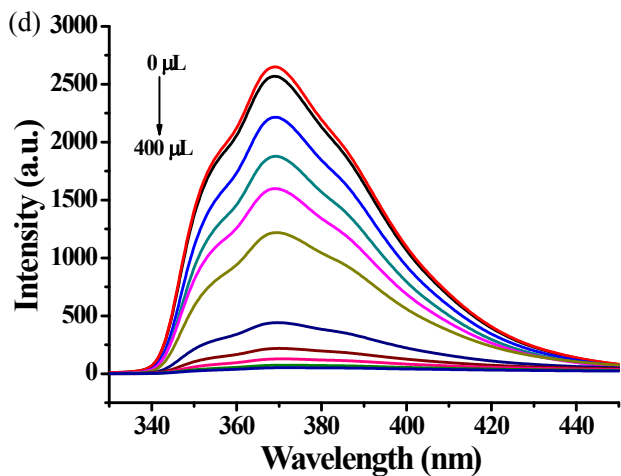


Figure S8. The curves of luminescence titration (a-e), and the plots of regression line (f-j) to calculate sensitivities of Fe^{3+} ion for **1-5**.

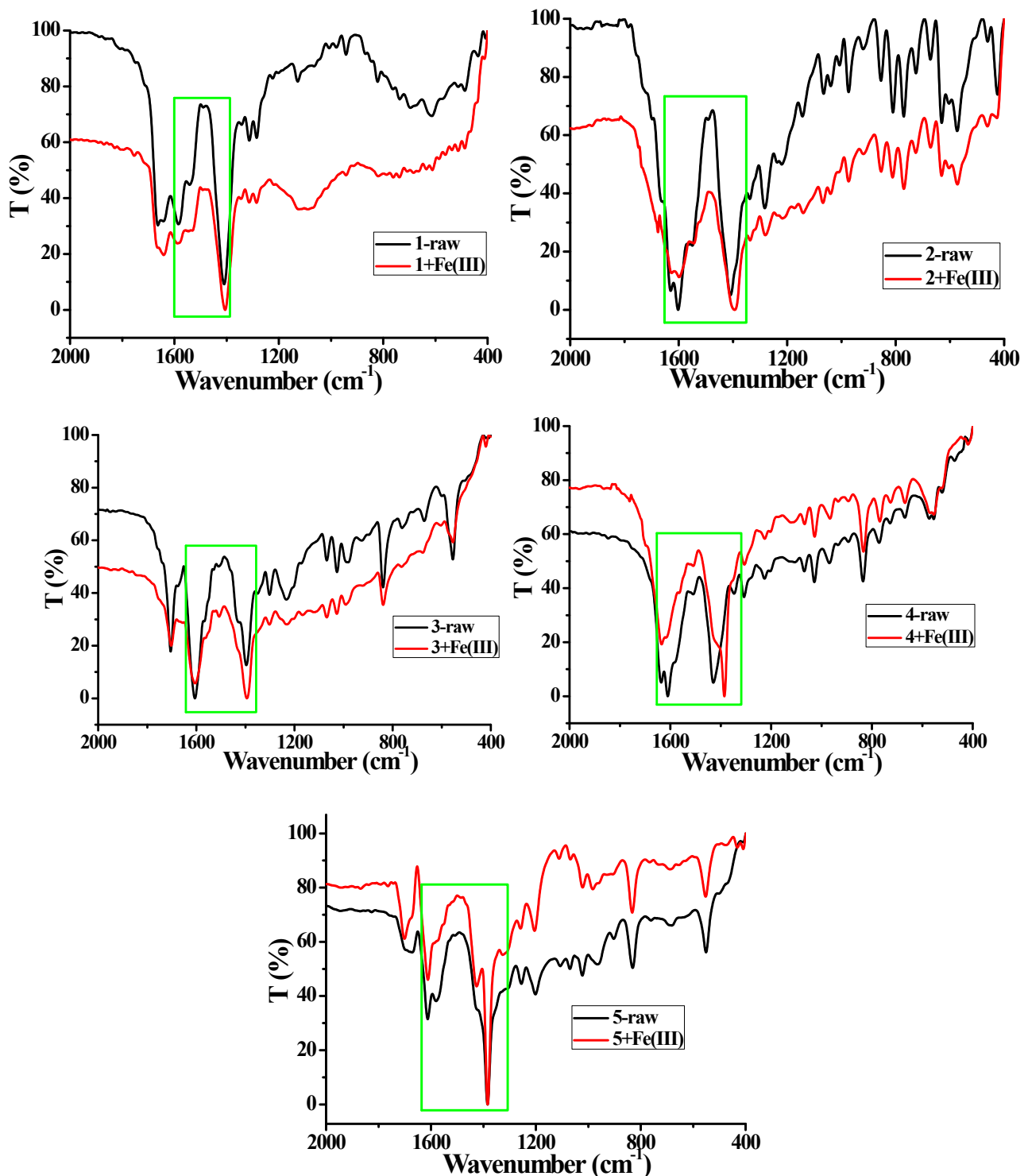


Figure S9. FTIR spectrum of the raw samples (black) and that after immersed in Fe^{3+} solution (red) for **1-5**. The green rectangle highlighted the differences of the stretching of carboxylate groups that coordinated to metals.

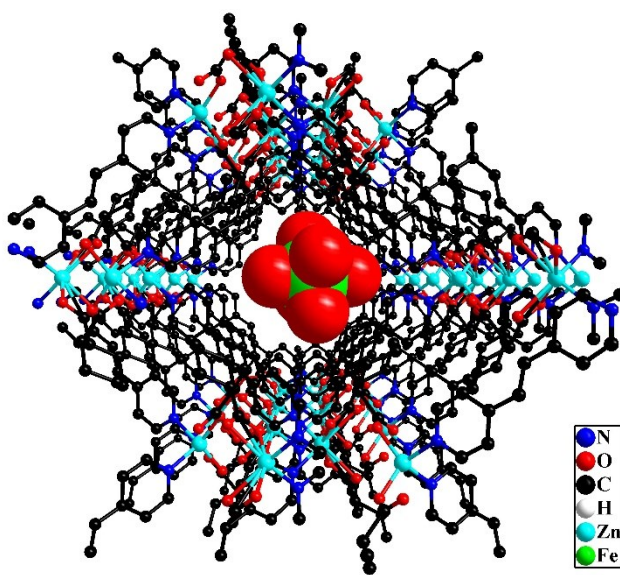


Figure S10. The most optimized adsorption site for $[\text{Fe}(\text{H}_2\text{O})_6]^{3+}$ groups trapped in the channel of **4** in solution.

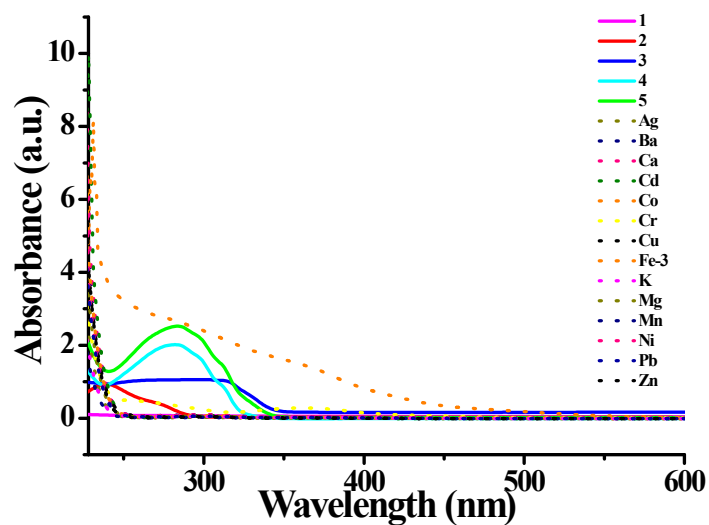


Figure S11. UV/vis spectra of **1-5** and metal ions used in titration experiments.

Table S1. Comparison of quenching constant K_{sv} and limit of detection (LOD) for various Zn-based fluorescent CPs used for detection of Fe^{3+} .

Materials	K_{sv} (M^{-1})	LOD	Solvent	Reference
[Zn(QDA)]·0.3DMF	1.12×10^6	0.023 μM	MeOH	<i>Dalton Trans.</i> , 2019, 48 , 1766-1773
[Zn(NIPH) ₂ (HPF) ₂]	6.062×10^5	15.5 ppb	DMSO	<i>Polyhedron</i> , 2020, 185 , 114605
ZSB-1	-	0.054 μM	DMF/isopropanol	<i>Small</i> 2018, 14 , 1703873
CSMCRI-1	2.54×10^4	1.29 μM	DMF	<i>ACS Appl. Mater. Interfaces</i> , 2019, 11 , 9042-9053
{[Zn(L)(bpe)]·DMF} _n	2.27×10^4	1.55 μM	DMF	<i>J. Solid State Chem.</i> , 2018, 261 , 75-85
[Zn ₃ (L) ₂ (bipy)(μ_3 -OH) ₂]·3H ₂ O	2.3×10^4	-	DMF / H ₂ O	<i>Sens. Actuators B</i> , 2018, 257 , 207-213
DUT-26	1.7×10^5	0.1 μM	DMF / H ₂ O	<i>New J. Chem.</i> , 2020, 44 , 11829-11834
{Zn ₂ (NO ₃) ₂ (4,4'-bpy) ₂ (TBA)} _n	7.48×10^3	7.18 μM	H ₂ O	<i>CrystEngComm</i> , 2019, 21 , 1948–1955
{[Zn(ATA)(L)]·H ₂ O} _n	5.57×10^2	3.76 μM	H ₂ O	<i>Inorg. Chem.</i> 2017, 56 , 10939-10949
[Zn ₃ (HL) ₂ (DMF) ₂ (H ₂ O) ₂]·2H ₂ O	2.05×10^5	-	H ₂ O	<i>J. Lumin.</i> , 2017, 188 , 346-355
[Zn ₂ (TPOM)(NDC) ₂]·3.5H ₂ O	1.9×10^4	2 μM	H ₂ O	<i>Inorg. Chem.</i> , 2017, 56 , 12348–12356
[Zn ₂ (4,4'-nba) ₂ (1,4-bib) ₂] _n	1.68×10^4	1.76 μM	H ₂ O	<i>New J. Chem.</i> , 2020, 44 , 4011-4022
[Zn ₂ (tpeb)(bpdc) ₂]·0.5DMA·4H ₂ O	1.326×10^4	0.882 μM	H ₂ O	<i>Inorg. Chem.</i> 2020, 59 , 8818–8826
[Zn(bimpy)(1,4-ndc)]·H ₂ O	1.02×10^4	0.882 μM	H ₂ O	<i>New J. Chem.</i> , 2020, 44 , 8728-8735
1	0.30×10^4	3.46 μM	H ₂ O	This work
2	0.60×10^4	2.46 μM	H ₂ O	This work
3	1.06×10^4	2.17 μM	H ₂ O	This work
4	1.03×10^4	2.65 μM	H ₂ O	This work
5	2.31×10^4	0.77 μM	H ₂ O	This work

Table S2. Crystal data and structure refinements for **1-5**.

	1 (293 K)	2 (150 K)	3 (120 K)	4 (100 K)	5 (120 K)
empirical formula	C ₁₀ H ₁₆ O ₁₂ Zn ₂	C ₁₅ H ₁₂ NO ₈ Zn ₂	C ₂₂ H ₂₀ N ₂ O ₈ Zn	C ₂₀ H ₂₆ N ₂ O ₇ Zn	C ₂₀ H ₂₅ N ₃ O ₉ Zn
<i>M</i>	458.97	465.00	505.77	471.82	516.80
wavelength (Å)	0.71073	1.54178	1.54178	1.54178	0.71073
crystal system	Monoclinic	Monoclinic	Orthorhombic	Orthorhombic	Triclinic
space group	<i>C</i> 2/c	<i>P</i> 2 ₁ /n	<i>P</i> bca	<i>P</i> nna	<i>P</i> -1
a/Å	12.2574(6)	8.6953(14)	9.8032(4)	25.1315(6)	8.1309(9)
b/Å	13.4329(6)	10.2001(11)	18.8923(8)	11.8428(3)	11.1211(11)
c/Å	18.4947(8)	16.7973(18)	22.6814(7)	15.9866(3)	12.0204(11)
α /°	90	90	90	90	82.746(8)
β /°	94.667(2)	104.530(12)	90	90	82.652(8)
γ /°	90	90	90	90	83.543(8)
Vol/Å ³	3035.1(2)	1442.2(3)	4200.7(3)	4758.05(19)	1064.25(19)
<i>Z</i>	8	4	8	8	2
ρ _{calcd} /g cm ⁻³	2.009	2.142	1.599	1.166	1.613
μ/mm ⁻¹	3.225	4.588	2.106	1.625	1.213
reflns collected	11128	3667	10450	12939	13650
unique reflns	3297(0.0550)	2227(0.0300)	4114(0.0658)	4586(0.0178)	4614(0.0462)
<i>S</i>	1.057	0.919	1.039	1.059	1.046
R ₁ ^a , wR ₂ ^b (<i>I</i> > 2σ(<i>I</i>))	0.0347, 0.0765	0.0314, 0.0655	0.0768, 0.2002	0.0617, 0.1989(squeeze)	0.0468, 0.1098
R ₁ ^a , wR ₂ ^b (all data)	0.0483, 0.0826	0.0445, 0.0682	0.1015, 0.2240	0.0697, 0.2106(squeeze)	0.0556, 0.1167

^a R₁ = ∑||F_o| - |F_c||/ ∑|F_o|, ^b wR₂ = [∑w(F_o² - F_c²)² / ∑w(F_o²)²]^{1/2}

Table S3. The hydrogen bonding list for **1**, **3** and **5**.

D-H...A	d(D-H)	d(H...A)	d(D...A)	<(DHA)
1				
O(1W)-H(1WA)...O(2Wd)	0.85	2.16	2.653(7)	116.9
O(1W)-H(1WA)...O(2W'd)	0.85	2.00	2.538(7)	120.6
O(1W)-H(1WB)...O(2W'e)	0.85	2.21	2.826(7)	129.2
O(1W)-H(1WB)...O(3W'f)	0.85	2.25	2.725(13)	115.6
O(2W)-H(2WA)...O(4c)	0.85	2.03	2.744(6)	141.8
O(2W)-H(2WB)...O(3)	0.85	1.97	2.696(6)	142.7
O(2W')-H(2WC)...O(3)	0.85	2.21	3.052(8)	172.2
O(2W')-H(2WD)...O(4c)	0.85	1.87	2.714(7)	172.2
O(3W)-H(3WA)...O(7d)	0.97	2.10	3.064(8)	170.2
O(3W)-H(3WB)...O(4W)	0.94	1.86	2.79(2)	168.1
O(3W)-H(3WB)...O(4Wb)	0.94	2.65	3.406(18)	137.8
O(3W')-H(3WC)...O(4W')	0.84	2.38	2.89(2)	119.8
O(3W')-H(3WD)...O(7D)	0.85	2.36	3.133(10)	151.4
O(4W)-H(4WA)...O(3)	0.85	2.04	2.890(9)	178.3
O(4W)-H(4WB)...O(6a)	0.85	2.08	2.933(9)	178.2
O(4W')-H(4WC)...O(6a)	0.85	2.51	3.307(11)	157.5
O(4W')-H(4WD)...O(7d)	0.85	2.42	3.227(11)	157.6
3				
O(4)-H(4B)...O(6a)	0.84	2.00	2.839(9)	174.8
O(4)-H(4B)...O(6'a)	0.84	1.93	2.71(2)	153.1
O(5)-H(5B)...O(3b)	0.84	1.80	2.636(6)	175.5
5				
O(1W)-H(1WA)...O(3a)	0.85	1.88	2.732(3)	178.6
O(1W)-H(1WB)...O(5)	0.85	1.86	2.670(3)	157.8
O(2W)-H(2WA)...N(3b)	0.85	2.62	3.449(3)	164.1
O(2W)-H(2WA)...O(6b)	0.85	2.55	3.276(4)	143.3
O(2W)-H(2WA)...O(7b)	0.85	2.05	2.867(3)	160.7
O(2W)-H(2WB)...O(7a)	0.85	1.92	2.739(4)	160.4
O(4)-H(4)...O(2W)	0.97	1.65	2.574(3)	159.3

Symmetry transformations used to generate equivalent atoms:

For **1**: a) $x-1/2, y+1/2, z$; b) $-x+2, y, -z+1/2$; c) $-x+5/2, y+1/2, -z+1/2$; d) $-x+5/2, -y+1/2, -z+1$; e) $x-1/2, -y+1/2, z+1/2$; f) $-x+2, -y+1, -z+1$.For **3**: a) $x-1/2, y, -z+3/2$; b) $x+1/2, y, -z+3/2$.For **5**: a) $-x, -y+1, -z+2$; b) $x, y-1, z+1$.